Two-body decay of thermalized excitons in Cu_2O

J. T. Warren, K. E. O'Hara, and J. P. Wolfe
Physics Department and Materials Research Laboratory, University of Illinois at Urbana-Champaign, 1110 West Green Street, Urbana, Illinois 61801

(Received 25 October 1999)

We have examined the decay of thermalized excitons in cuprous oxide (Cu_2O) and determined their lifetime against two-body decay (i.e., Auger recombination). The experiments are conducted at $T=70$ K with near-resonant picosecond excitation to ensure a thermal equilibrium between orthoexcitons, paraexcitons, and the crystal lattice. Time-resolved spectroscopy reveals the gas reaching equilibrium with the lattice temperature in 0.5 ns. The wavelength of the excitation photons and the spatial distribution of the laser beam are selected to produce a well defined spatial distribution of excitons. Time-resolved photoluminescence imaging measures the diffusion of excitons. From absolute measurements of the gas volume and the luminescence intensity, we determine the instantaneous gas density. At high excitation levels, a rapid nonexponential decay of the excitonic gas is observed. The decay curve is well explained by assuming that the local exciton density is governed by the rate equation $dn/dt=-An^2-n/\tau$, with an Auger constant $A=0.6\times10^{-16}$ cm^3/ns and a residual decay time $\tau=300$ ns. This value of the Auger constant is comparable to that estimated previously for a nonthermalized exciton gas at a lattice temperature of 2 K, indicating that the Auger lifetime of an exciton is only weakly dependent on its kinetic energy. The Auger process characterized here defines the practical limits for exciton densities in cuprous oxide.

I. INTRODUCTION

Photons with energies greater than the energy gap E_{gap} of a semiconductor create electron-hole pairs within the absorption length of the incident light in the crystal. The fate of the electrons and holes depends upon many factors. Their initial kinetic energy is shed by phonon emission, and at sufficiently low temperatures they combine into bound electron-hole pairs, or excitons. The excitons diffuse out of the initial excitation volume at a rate dependent on their energy and mobility. The intrinsic lifetime of an exciton — due to radiative decay of the electron-hole pair — depends primarily on the crystalline band structure, but the actual lifetime is often limited by electron-hole recombination at defects.

In the present paper, we examine an important density-dependent contribution to the exciton lifetime. This two-body process, known as exciton annihilation or Auger recombination, involves the collision of two excitons in which the nonradiative recombination of one electron-hole pair transfers kinetic energy to the remaining electron and hole.[1] The instantaneous Auger decay rate for an exciton equals An, where A is the Auger constant and n is the density of the exciton gas. Auger decay is a common process for high density electron-hole plasmas and in the electron-hole liquid,[2,3] but this decay route is not common for free excitons because their densities are typically much lower than the plasma densities. Cuprous oxide (Cu_2O) is an exception.

Compared to excitons in other semiconductors, the excitons in cuprous oxide are relatively simple.[4] Spherical electron and hole bands and relatively large carrier masses produce an excitonic binding energy of 150 meV and Bohr radius of about 0.7 nm. The band structure precludes the formation of biexcitons or electron-hole droplets. Also, cuprous oxide possesses a forbidden direct gap, implying relatively long lifetimes against radiative recombination and correspondingly weak photoluminescence from the excitons. With focused excitation pulses, it is possible to produce sufficiently high densities of excitons that two-body decay processes become dominant.

These qualities have promoted the exciton in Cu_2O as a candidate for Bose-Einstein condensation (BEC).[5–7] Indeed, it was the search for BEC in Cu_2O that revealed the existence of an Auger process in this crystal.[8,9] It is widely believed that the Auger process is the principal process that limits the exciton density, yet a systematic quantitative measurement of this two-body decay mechanism has proved elusive. Recent experiments by our group[10,11] have concentrated on measuring this process and found it to be much stronger than estimated earlier, calling into question the claims of quantum statistics of excitons in this semiconductor. The present paper puts the absolute measurement of the Auger constant A on a firmer basis.

One complication of cuprous oxide is that the excitonic ground state has a large exchange splitting. This interaction causes the $1s$ state (with spin-1/2 electron and hole) to split into a singlet (the paraexciton) and a triplet (the orthoexciton) lying 12 meV higher. Orthoexciton-to-paraexciton conversion by phonon emission plays an important role in the thermalization of the excitons.[12–15]

The experimental challenge in measuring the Auger constant is to separate the two-body decay rate from (1) the single-exciton decay rate, (2) the rate at which the exciton density decays due to exciton diffusion, (3) the orthoexciton-to-paraexciton conversion rate, and (4) the time-resolution limits of the laser pulse and photon detection system.

To overcome these difficulties, we use a lattice temperature[16] of 70 K (higher than in the experimental attempts at Bose-Einstein condensation) and 6-ps laser pulses. At 70 K, the excitons thermalize within 0.2 ns and orthoexciton-to-paraexciton conversion reaches equilibrium

within 0.1 ns.[13] A stabilization of the gas temperature during the measurement is crucial because orthoexciton decay due to orthoexciton-to-paraexciton conversion may depend on the gas temperature. For an equilibrated gas, the orthoexciton signal (what we measure) is proportional to the *total* exciton population, allowing a straightforward determination of A. Also, the lifetime of this thermalized orthoexciton/paraexciton system in our sample at 70 K is long, $\tau = 300$ ns, limited by recombination at impurities and defects.[17] This long decay time permits long observation times for the Auger process.

We measure the Auger decay rate by observing the decay in exciton density. Ignoring exciton diffusion, the local decay of a single-component excitonic gas with density $n = n(\mathbf{r},t)$ in Cu_2O is described by the following rate equation:

$$dn/dt = -n/\tau - An^2 + G, \tag{1}$$

where τ is the single-body decay time at low density, A is the Auger decay constant, and $G = G(\mathbf{r},t)$ is the optical generation rate. Experiments create a nonuniform gas of excitons, and excitons diffuse, so the analysis of the decay processes must take into account (a) spatial inhomogeneity and (b) exciton diffusion.

To address the spatial problems, we carefully select the excitation volume. The wavelength of a picosecond dye laser is chosen to produce an appropriate absorption length l and an expanded laser beam is apertured and imaged onto a disk-shaped area on the crystal surface, in order to produce a constant density over the excitation area. The analytic form of the exciton density $n(z,t)$ in the Auger regime is derived for this excitation geometry in the absence of particle diffusion. We show that at 70 K, the exciton diffusivity is 7.6 cm^2/s [30 times slower than at 2 K (Ref. 18)] so the volume expansion of the gas is minimized. For all of the above reasons (rapid exciton thermalization, relatively long single-body decay time, and slow exciton diffusion) the measurement of the Auger process is best attempted at the higher temperature. In Sec. VI we discuss evidence that this process is not strongly dependent on crystal temperature.

This paper is organized as follows. In Sec. II we describe a simple but effective model for the Auger decay of excitons produced by near-surface excitation, taking into account the spatial inhomogeneities in the optical generation rate. In Sec. III we use time-resolved spectroscopy to characterize the thermalization of exciton energy following picosecond resonant excitation at 70 K. In Sec. IV we describe the results of our time-resolved spatial imaging experiments to determine the diffusivity of the excitons. In Sec. V we analyze the decay of the exciton luminescence under controlled spatial conditions to determine the Auger constant. Our conclusions are presented in Sec. VI.

II. MODELING AUGER DECAY

The principal effect of the two-body collision process is to reduce the lifetime of the excitonic gas at high densities. A secondary effect, which becomes important at low lattice temperatures (e.g., $T = 2$ K) is the heating of the excitonic gas due to the kinetic energy produced by Auger events. However, if the lattice is held at 70 K, the Auger-heating effect is counteracted by the rapid gas cooling via exciton-phonon scattering. Therefore, in this section we present a model that assumes the excitonic gas is thermalized to the lattice temperature, an assumption that is experimentally verified in the following section.

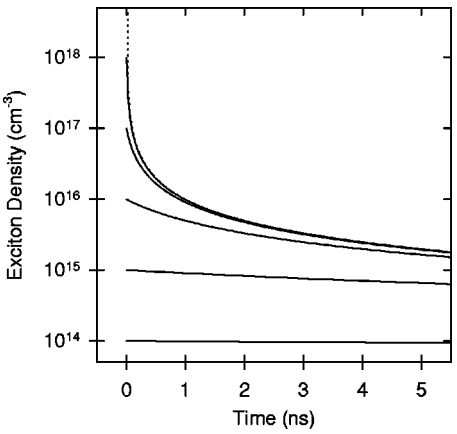

FIG. 1. Decay of exciton densities $n(t)$ predicted by Eq. (3) for a spatially uniform gas of excitons. The calculations assume an Auger constant $A = 10^{-16}$ cm^3/ns, a single-particle decay time $\tau = 300$ ns, and initial densities n_0 ranging from $10^{14}/cm^3$ to $10^{18}/cm^3$.

If the orthoexciton-to-paraexciton interconversion rate is fast compared to the overall decay rate, we may consider a rate equation like Eq. (1), where n represents the total ortho-plus-para exciton density. However, we must consider the meaning of A in that equation. Conceptually there are three distinct Auger constants, A^{oo}, A^{op}, and A^{pp}, depending on the colliding species, orthoexcitons (o) or paraexcitons (p). In the experiments described here we cannot isolate the individual processes because of the fast interconversion. (Also the weak paraexciton signal is obscured by a much stronger orthoexciton phonon replica.) At a temperature of 70 K, 71% of the excitons are paraexcitons, so the experiments actually measure the combination,

$$\begin{aligned} A &= (o^2/n^2)A^{oo} + 2(op/n^2)A^{op} + (p^2/n^2)A^{pp} \\ &= 0.08A^{oo} + 0.41A^{op} + 0.51A^{pp}, \end{aligned} \tag{2}$$

where o and p represent the orthoexciton and paraexciton densities and $n = o + p$. In Sec. VI we will comment further on the separate processes.

First consider an excitonic gas that is homogeneous in space created by an optical pulse that is a δ function in time. The decay of the exciton density from its initial value n_0 is governed by Eq. (1) with $G = 0$. The solution is

$$n(t) = \frac{n_0 e^{-t/\tau}}{1 + An_0\tau(1 - e^{-t/\tau})}. \tag{3}$$

To see the form of this function, we assume $A = 10^{-16}$ cm^3/ns and plot $n(t)$ in Fig. 1 for initial densities ranging from $1\times10^{14}/cm^3$ to $1\times10^{18}/cm^3$. No matter how high the initial density n_0, the instantaneous density $n(t)$ is bounded by

$$n(t) = \frac{1/A\tau}{e^{t/\tau} - 1}. \tag{4}$$

This limiting function is plotted as the dotted trace in Fig. 1. In the present example, increasing the initial gas density to levels higher than about $1\times10^{17}/\mathrm{cm}^3$ has almost no effect on the instantaneous densities at times beyond 1 ns.

In a realistic experiment, the optical generation rate is $G(z,t)=G_0(t)\exp(-z/l)$, where z is the displacement normal to the crystal surface and l is the optical absorption length at the wavelength chosen. The experiments integrate the luminescence signal along a direction normal to the surface.

For a δ-function excitation pulse, this exponentially decreasing generation rate is modeled by integrating the homogeneous solution, Eq. (3) but with $n_0(z)=n_s\exp(-z/l)$, where n_s is the initial volume density at the sample surface. This initial condition yields an *areal* density of excitons given as a function of time by

$$n_a(t)\equiv\int n(t)\,dz=\frac{l}{A\tau}\frac{\ln[1+An_s\tau(1-e^{-t/\tau})]}{e^{t/\tau}-1}. \quad (5)$$

This equation is plotted in Fig. 2(a) for $A=10^{-16}$ cm^3/ns and initial surface densities ranging from $1\times10^{14}/\mathrm{cm}^3$ to $1\times10^{18}/\mathrm{cm}^3$.

Figure 2(a) shows that the effect of the exponentially decreasing generation function is significant. Unlike the homogeneous case, the exciton density integrated along the z axis at a given time continues to increase with increasing power because, as the density of excitons near the surface saturates, excitons from less dense regions contribute more effectively to the spatial integral. This implies that as the generation rate is increased, the spatial profile $n(z)$ at a given time becomes broader. The development of this broadening with time is shown in Fig. 2(b), which plots Eq. (3) at discrete times, with the initial density n_0 proportional to $\exp(-z,l)$.

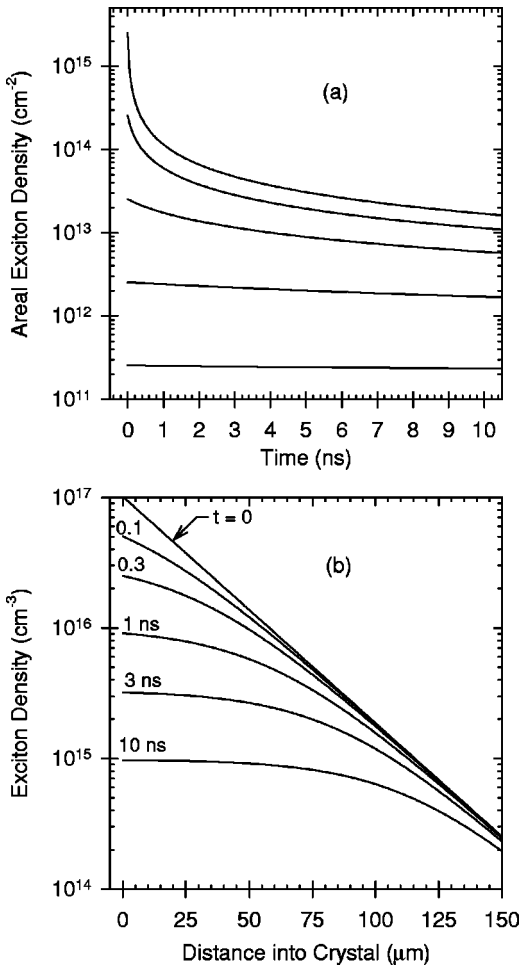

FIG. 2. (a) Decay of the exciton areal densities $n_a(t)$ predicted by Eq. (5) for a spatially varying gas of excitons, produced by an exponentially decreasing generation rate. The calculations assume an Auger constant $A=10^{-16}$ cm^3/ns, an absorption length $l=25$ μm, a single-particle decay time $\tau=300$ ns, and initial densities n_s ranging from $10^{14}/\mathrm{cm}^3$ to $10^{18}/\mathrm{cm}^3$. (b) Spatial distribution of excitons, at various times after creation with $n_s=10^{17}/\mathrm{cm}^3$.

III. THERMALIZATION OF THE EXCITON GAS

The choice of excitation wavelength affects both the excess kinetic energy imparted by the incident photons to the carriers and the absorption length of the light. We require an absorption length small enough that densities in the Auger regime can be achieved, and large enough that the excitons will not significantly diffuse out of this region during the Auger decay process. To make this choice, we carefully examine the absorption spectrum of Cu_2O near the semiconducting band edge.

Figure 3 shows the absorption spectrum of a thin (50 μm) crystal of Cu_2O at 70 K. The experiment measures the ratio α/n of the absorption coefficient to the refractive index by observing the transmission and the spectral spacing between interference fringes. The left scale of the figure can be converted to $\alpha=1/l$ by multiplying by the refractive index $n\sim3.0$ at this wavelength.[19] The *direct* creation of an orthoexciton occurs at a photon energy 2025.2 meV and is too weak to be observed on this scale. The onsets of the phonon-assisted orthoexciton absorption bands are at $h\nu=2011.6$ meV (Stokes) and 2038.8 meV (anti-Stokes). The resonances corresponding to the $n=2$ to $n=7$ Rydberg states of the excitons are labeled in Fig. 3(b) and a fit to the peak energies, shown in Fig. 3(c), yields a Rydberg of 94.7 meV and a band-gap energy equal to 2164.9 meV by taking the $n\to\infty$ limit. Note that the $1s$ exciton binding energy is not equal to this Rydberg due to central cell corrections. Also, the lowest-lying exciton state (paraexciton) lies 12.0 meV below the orthoexciton; its binding energy is 151.7 meV.

We choose not to directly pump one of the resonant lines because small shifts in lattice temperature would cause an undesirable significant change in the absorption length of the light (and thus the exciton density). Instead we pump with a photon energy of 2165 meV, corresponding to a wavelength of 572.5 nm, creating free electrons and holes very near the band edge. Assuming an index of refraction of 3, the absorption length at this wavelength is 25 μm. This value is small enough to achieve sufficient densities to observe Auger decay, while it is significantly larger than the mean diffusion distance of the excitons during their rapid two-body decay, as we will show in the next section.

To observe the energy relaxation of the excitons produced with this excitation light at 70 K, we switch to a thick mineral sample [a 2.5-mm cube with (100) faces] and employ the experimental setup to be used in our Auger measurements sketched in Fig. 4(a). A cavity-dumped mode-locked

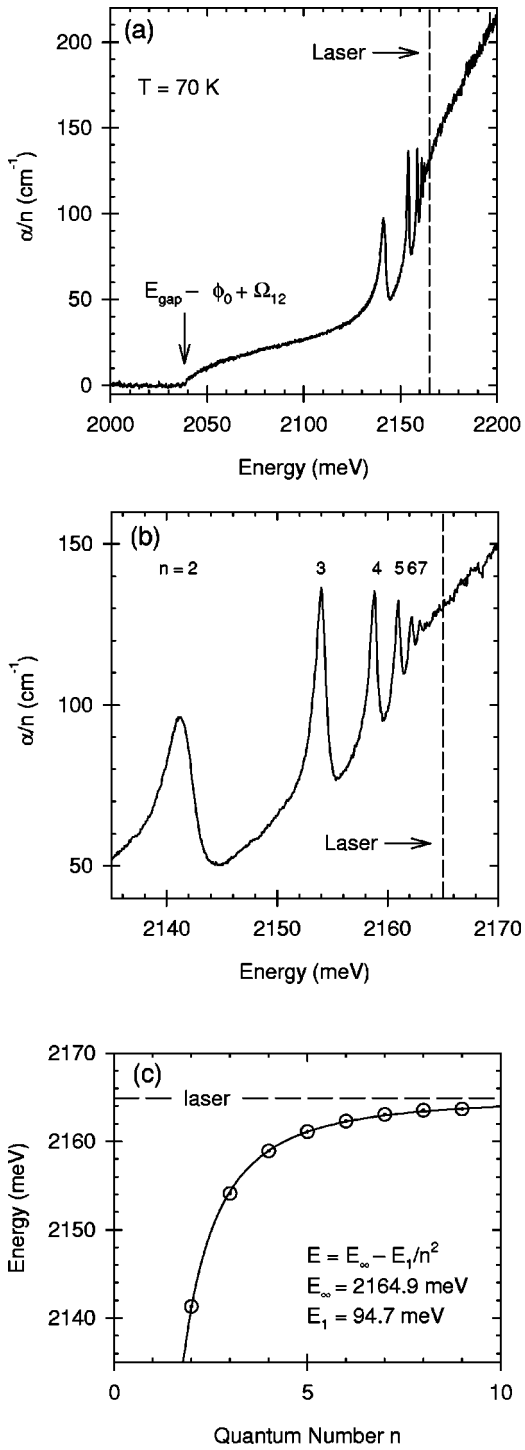

FIG. 3. (a) Absorption spectrum of a 50-μm-thick mineral crystal of Cu_2O at 70 K. Plotted is the absorption coefficient divided by the index of refraction of the crystal, $n \approx 3$. The onset of the strong anti-Stokes phonon-assisted orthoexciton absorption band is at $h\nu = E_{gap} - \phi_{1s} + \Omega_{12} = (2164.9 - 139.7 + 13.6)$ meV $= 2038.8$ meV. (b) Expanded region of photon energy showing the excitonic Rydberg series and the chosen photon energy for the experiments described in this paper. (c) Energy positions of the excitonic absorption lines superimposed on the $1/n^2$ Rydberg function. The chosen photon energy for our experiments is at the $n = \infty$ level.

dye laser produces 5-ps pulses with energies up to 2.8 nJ. The pulse repetition time is typically 526 ns. The center of the laser beam is selected by a disk-shaped aperture and projected onto the sample surface. The excitation area is a disk

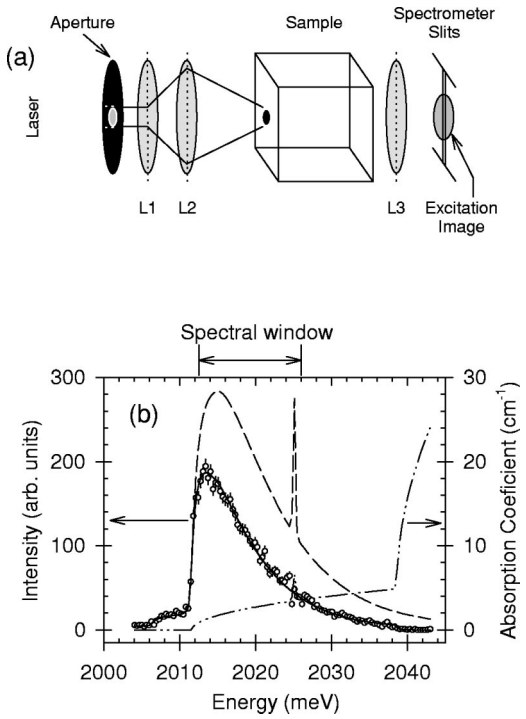

FIG. 4. (a) Excitation geometry, not to scale. The sample surface is *not* at a laser beam waist, rather it is in a position where geometrical ray optics describes the beam well. (b) Dots represent the phonon-assisted luminescence spectrum of orthoexcitons at 70 K. The solid curve through the data is a 70 K Maxwellian (dashed trace) diminished by the absorption of the luminescence light through the 2-mm-thick crystal. The dot-dashed line is the absorption coefficient from Fig. 3(a). A broad exit slit of the spectrometer is used for the spatial imaging experiments of Sec. III, and the corresponding spectral acceptance window is shown.

52 μm in diameter, as verified by spatially imaging the photoluminescence. The photoluminescence is passed through a 0.5-m spectrometer with a 1200 lines/mm grating used in first order. The light is detected with a microchannel-plate photomultiplier, and single-photon counting provides an overall time response of 70 ps, the measured full width at half maximum of the system's response to the 5-ps laser pulse. The optical efficiency of this system is calibrated so that we can determine the number of photons emitted per second from the excitation region. This rate is converted to an absolute number of excitons using the known radiative rate for an orthoexciton.[11]

The dots in Fig. 4(b) show a typical luminescence spectrum recorded at a time of 0.625 ns after the laser pulse. Plotted under the data is the absorption curve.[11] The solid curve is a fit to the data by a Maxwell-Boltzmann distribution (dashed curve) reduced by the wavelength-dependent absorption of the luminescence light collected through the crystal.[20] Excellent agreement is obtained for a fit temperature $T = 69$ K. Note that neglecting to take the absorption into account causes a narrower emission spectrum than expected for a Maxwell-Boltzmann distribution at the lattice temperature. This effect would become even more obvious at higher lattice temperatures. Also indicated in this figure is the spectral acceptance window chosen for the imaging experiments described in the next section.

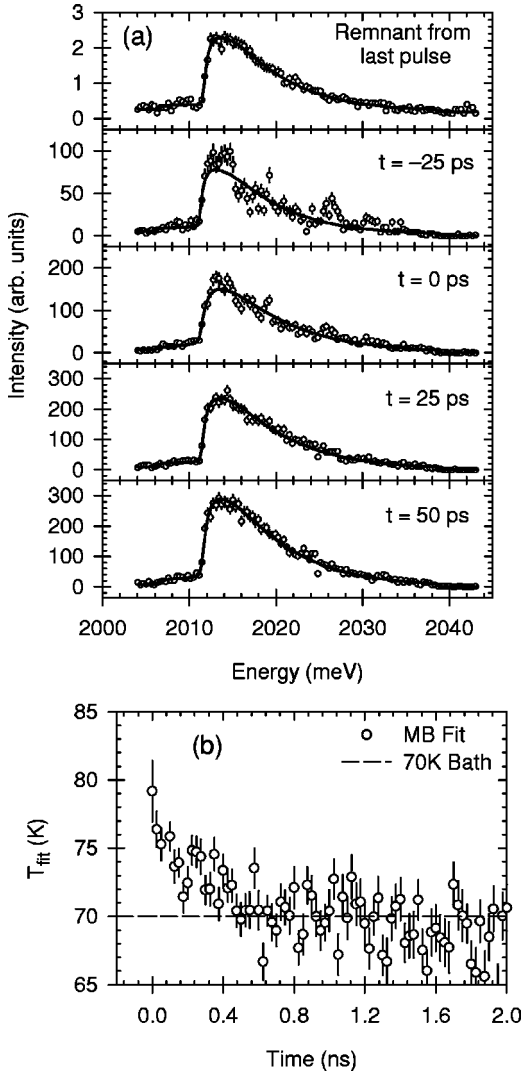

FIG. 5. (a) Time-resolved luminescence spectra of orthoexcitons following a 5-ps laser pulse depositing 2.9×10^7 photons/pulse. Solid curves are Maxwell-Boltzmann distributions. (b) The temperatures of those Maxwell-Boltzmann distributions as a function of time. The time scale is greatly expanded compared to later time plots in this paper. The excitons reach thermal equilibrium with the lattice within about 0.5 ns.

Figure 5(a) shows how the spectrum changes at various times after the excitation pulse. Note the scale changes. The uppermost data are an average over many time channels showing on an expanded intensity scale the remnant signal from the previous laser pulse. The solid curves are fits to Maxwellian distributions corrected for absorption. In Fig. 5(b), the resulting fit temperatures are plotted as a function of time. Most of the excess kinetic energy imparted by the laser photons is lost within the 50-ps response time of our detection system. The exciton gas temperature is within 2 K of the bath temperature after only 0.5 ns. The asymptotic fit temperature of the excitonic gas is about 68 K, close to the 70 K bath temperature shown as the horizontal dashed line in Fig. 5(b). We conclude that, for the purposes of the present work, the kinetic energies of the excitons are in thermal equilibrium with the lattice.

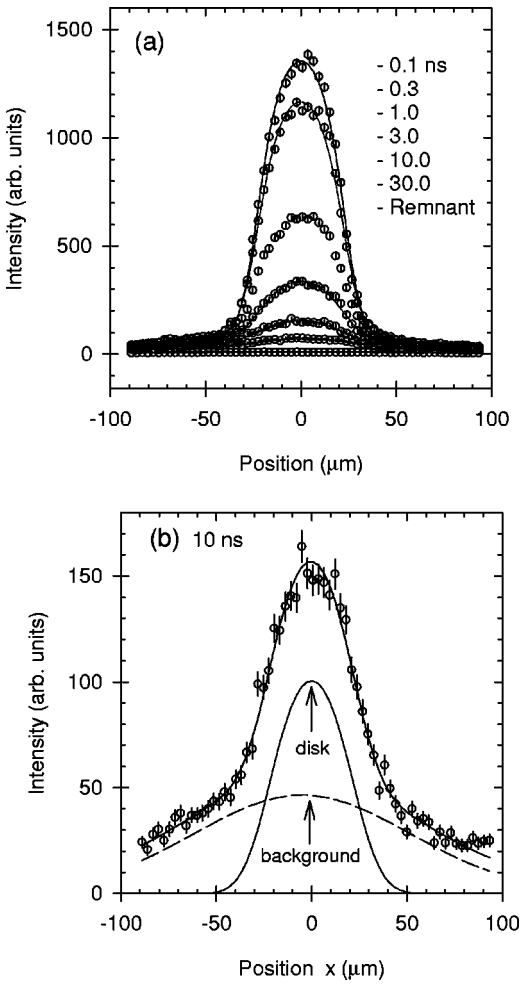

FIG. 6. (a) Time-resolved spatial profiles of the orthoexciton luminescence produced in a disk-shaped region of the crystal. The shapes of the early-time profiles agree well with the theoretical form given by Eq. (6). (b) Dots are an expanded view of the profile at $t=10$ ns. The data require a ''disk'' component and a ''background'' component, as described in the text. Solid curve is the composite fit.

IV. DESCRIBING THE EXCITON PROFILE

The spatial distribution of excitons is observed by scanning an image of the luminescent exciton cloud across the vertical entrance slit of the spectrometer. Time-resolved spatial profiles are shown in Fig. 6(a). In principle, the intensity passing through a narrow slit that is translated across a uniformly illuminated disk of radius R is given by

$$I=I_0\sqrt{1-(x/R)^2}. \tag{6}$$

The observed luminescence profiles fit this function very well at early times. Figure 6(b), however, shows that this ''disk luminescence'' is riding on top of a significant ''background'' luminescence.

The background luminescence originates from two sources: (a) excitons remaining from the previous pulse and (b) excitons produced by diffuse wings in the laser profile. The latter contribution, which rises in time with the laser pulse, is most likely due to a low density of excitons created by scattered and multiply reflected laser light. The background luminescence from these two sources is more promi-

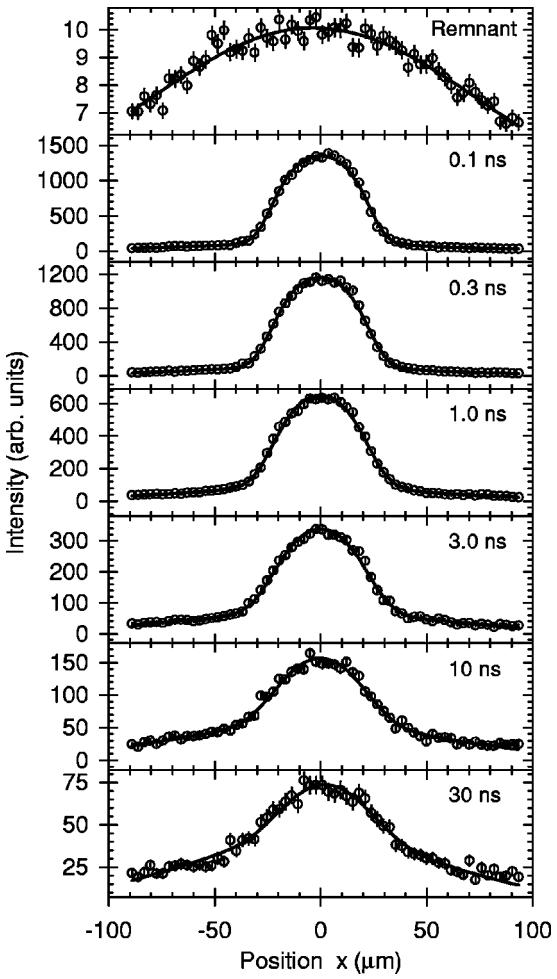

FIG. 7. Time-resolved spatial profiles from Fig. 6(a), normalized to the same height, showing the excellent fits to the disk + background function. The disk radius is unchanging in these fits, but the broadening of this function gives the diffusion distance of the excitons plotted in the next figure.

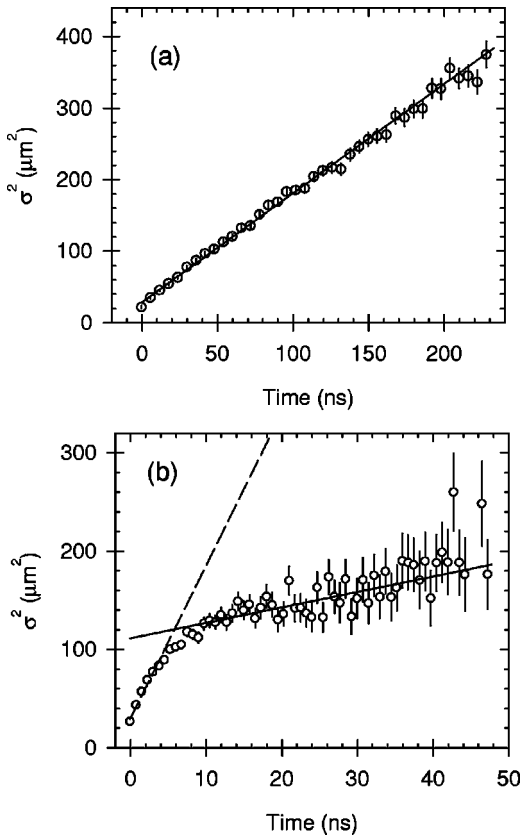

FIG. 8. (a) Square of the width of the Gaussian broadening convolved with the disk function. Data are taken at low excitation level, 2.9×10^7 photons/pulse, and the straight line gives $D=7.6$ cm^2/s. (b) Apparent rapid diffusion following the pulse at high excitation level, 5.1×10^9 photons/pulse. In fact, the rapid initial rise in σ^2 is due to the density-dependent Auger lifetime of the gas, not diffusion. The late-time expansion slope is the same as in part (a).

nent at late times because Auger recombination has reduced the number of excitons in the high-density disk region. The long (2 mm) vertical slit, chosen to safely include the entire excitation disk, also captures a large amount (400 μm) of this background.

The analysis of disk and background components is illustrated in Fig. 6(b), recorded at 10 ns after the laser pulse. The background is well modeled by a broad Gaussian distribution, $\exp(-x^2/2\sigma_b^2)$. Both components are convolved with a much narrower Gaussian, $\exp(-x^2/2\sigma^2)$, that accounts for our spatial resolution and the diffusion of excitons out of the excitation region. The radius of the disk is precisely determined by early-time and by low-density profiles (both giving $R=26\pm1$ μm) so the diffusive broadening can be confidently extracted. Figure 7 shows excellent fits to the data at all measurement times. As with the spectral data, the uppermost trace is an average over many time channels prior to the pulse and shows the remnant exciton cloud 524 ns after the previous laser pulse. (Note the low intensity.) The disk-shaped cloud rises to its peak intensity in 50 ps and decays more slowly due to recombination and diffusion of excitons out of the excitation region.

The broadening of the luminescent disk, as characterized by the Gaussian width σ, is plotted as a function of time in Fig. 8. At an excitation level of 2.9×10^7 photons per pulse [Fig. 8(a)] the data are fitted very well to the form $\sigma^2=\sigma_0^2+\sigma_d^2$, where $\sigma_0=4.7$ μm equals the optical resolution of the system, and $\sigma_d^2=2Dt$ represents the diffusion of excitons. We measure $D=7.6$ cm^2/s. It is now obvious why the choice of a lattice temperature of 70 K is important; at 2 K, the diffusion constant is 600 cm^2/s.[18] Such rapid expansion would hardly allow a constant-volume experiment.

At a higher excitation level of 5.1×10^9 photons per pulse, a rapid rise in σ^2 appears at early time, as shown in Fig. 8(b). This fast increase in width is better understood as a fast *decrease* in *height* of the distribution, due to Auger decay. Despite our best efforts to create an exciton distribution with sharp boundaries (in the x-y plane) the distribution will have some wings due to laser spot imperfections, the finite numerical aperture of the laser beam, and normal diffusion of excitons. While these broadening influences are small, the high-density exciton gas in the center of the region decays quickly through Auger decay, making these wings relatively more prominent, and the best-fit σ larger. Once the initial distribution has settled down, the excitons are observed to diffuse with $D=7.6$ cm^2/s as in the low-density case.

The region of the excitation area least affected by the optical resolution and diffusion is that at the disk's center, $r=0$. Therefore, to minimize the effects of diffusion and wings in the excitation distribution, we choose to extract the exciton areal density here, $n_a(r=0)$, as a function of time. Then we will use this information to determine the Auger constant.

Rather than try to select the center of the excitation region with optical masking, we chose to extract the areal density at $r=0$ from our time-resolved slit scans of the entire excitation region. The slit scans are quite well fitted by the ''broadened disk'' plus the ''background'' components described above, so if N is the number of excitons in the ''broadened disk'' then the areal density at the center of the disk is

$$n_a(r=0)=\frac{N}{\pi R^2}(1-e^{-R^2/2\sigma^2}). \tag{7}$$

The equation above is simply the convolution of a two-dimensional disk with a Gaussian, evaluated at the origin.

V. MEASUREMENT OF THE AUGER DECAY RATE AT 70 K

Having chosen experimental conditions where thermalization effects and shape changing effects are minimal, we proceed to a measurement of the Auger rate. The signal at the center of our $R=25$ μm disk is nearly independent of the edge effects (i.e., diffusion), so this measurement corresponds to the one-dimensional model leading to Eq. (5). Our principal results are shown in Fig. 9. The dots are the areal densities calculated from our time-resolved slit scans using Eq. (7).

The lowest excitation level, 2.9×10^7 photons absorbed per pulse, corresponds to an areal density of absorbed photons equal to 1.5×10^{12} photons/cm^2. The initial luminescence brightness indicates 2.3×10^{12} excitons/cm^2 [including both orthoexcitons and paraexcitons, and correcting for reabsorption of luminescence and for the finite spectral acceptance depicted in Fig. 4(b)]. We trust the calibration of our spectrometer and optical collection system to within a factor of 2, but of course at most one exciton can be created for each photon absored, while our calibration and the observed luminescence indicate 1.5 excitons per photon absorbed. We will present and analyze the experimental results in terms of excitons *observed*, knowing that the observed numbers are overestimates, and return to consider this systematic error at the end of the analysis.

The lowest excitation level in Fig. 9(a) produced an initial density distribution $n_s\exp(-z/25\ \mu\text{m})$, where the observed luminescence indicates $n_s=1.0\times10^{15}$ excitons/cm^3 initially. On the time scale of Fig. 9(a), the decay rate of the excitons appears to be nearly exponential. However, the initial decay rate is about $(40\ \text{ns})^{-1}$ and the rate approaches $(300\ \text{ns})^{-1}$ at long times, which is the decay rate we measure in very low-density exciton gasses. Two-body decay is already effective at this low initial density.

As the excitation level is raised to 4.0×10^8 photons/pulse, the decay rate at $t=1$ ns quickens to about $(6\ \text{ns})^{-1}$, forty times larger than the single-particle decay rate. As predicted in the calculations of Fig. 2, two-body decay is strongly governing the loss of excitons. For the highest excitation level of 5.1×10^9 photons/pulse, the Auger effect is immense. The decay rate at $t=1$ ns is about $(1\ \text{ns})^{-1}$.

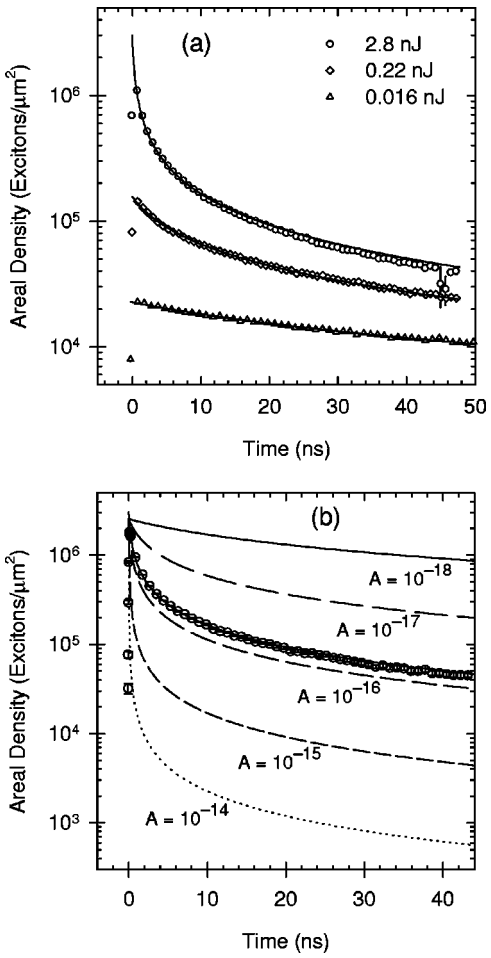

FIG. 9. (a) Decay of the luminescence n_a at the center of the disk profile for three different excitation levels. The rapid decay at high density is due to the two-body decay process. The solid curves are fits to the areal density formula, Eq. (5), with $A=6.5$, 5.5, and 4.8×10^{-17} cm^3/ns for the high, medium, and low excitation levels, respectively. (b) Dots show the areal density decay at the highest excitation level on an expanded time scale. Dashed curves are predictions for the designated values of A, and the solid curve represents the best-fit value of the Auger constant, 6×10^{-17} cm^3/ns.

The solid curves in Fig. 9(a) are best fits of Eq. (5) to the data, yielding Auger constants $A=6.5$, 5.5, and 4.8×10^{-17} cm^3/ns for the high, medium, and low excitation levels, respectively. Therefore, over two orders of magnitude in density, a consistent value of A is obtained. The high- and medium-power measurements have a higher confidence level. In each case, the single-particle decay time is taken to be 300 ns, as determined from low-power experiments. From these data, our best estimate of the Auger constant is

$$A=0.6\times10^{-16}\ \text{cm}^3/\text{ns} \tag{8}$$

with uncertainty dominated by the uncertainty in initial exciton density. If the initial density were a factor of 2 lower (the uncertainty in this type of calibration), the value of A

would increase to 1.2×10^{-16} cm^3/ns. This number relies on our density calibration, and the error bars reflect our confidence in this measurement. Figure 9(b) demonstrates the sensitivity of the excitonic decay curves to the Auger constant.

VI. CONCLUSIONS

As mentioned earlier, the Auger rate may depend upon whether the colliding particles are orthoexcitons or paraexcitons. The relation between the overall Auger rate, which we measure, and the individual rates is given by Eq. (2) for a thermalized gas of excitons. Because the density ratio of orthoexcitons to paraexcitons in thermal equilibrium, $o/p = 3\exp(-12 \text{ meV}/k_BT)$, decreases rapidly with temperature, the paraexciton-paraexciton contribution would dominate A at lower temperatures. Below about 15 K, however, the above function for o/p is not applicable because the orthoexciton- to-paraexciton conversion rate decreases with temperature and the photoexcited orthoexcitons do not reach thermal equilibrium with paraexcitons during their lifetime.[12] Below 15 K, the orthoexciton single-body decay time is determined by orthoexciton-to-paraexciton conversion.

Prior experiments in our group have provided mixed conclusions about the Auger decay of paraexcitons in Cu_2O at low temperatures. Lin and Wolfe[21] reported a slow decay of paraexcitons following a 10-ns Ar^+ laser pulse. More recent work[11] also shows a slow decay after the pulse, but the small paraexciton intensities indicate that the paraexcitons do indeed suffer from Auger decay. O'Hara and Wolfe[22] have recently calculated the thermalization of orthoexcitons and paraexcitons, including the known rates of phonon-exciton scattering, orthoexciton-to-paraexciton conversion, and spatial diffusion, and their results using $A^{oo}=A^{op}=A^{pp}$ are in agreement with the experimental results of Ref. 11.

An important issue is the temperature dependence of the two-particle decay process. Unlike elastic scattering, we do not expect the Auger rate to have the form $n^2\sigma_A v$, where n is the density, σ_A the Auger cross section, and v the particle velocity. Auger decay is different from elastic scattering in that the density of final states is not proportional to the initial velocity of the particles. The ionized electron and hole can reach a large volume of phase space because they share an amount of kinetic energy equal to the band gap. This argument suggests that the Auger constant may be relatively independent of the initial velocity of the excitons and thus relatively independent of temperature.

An earlier experiment (Ref. 11) estimated the two-body decay of orthoexcitons at 2 K under quite different excitation conditions than the present experiments. A 200-ps green laser pulse with absorption length of 3 μm was focused to a 10-μm spot. The kinetic energy of the orthoexcitons varied considerably during the measurement, and a rapid exciton diffusion had to be taken into account in estimating the exciton density. At 2 K the orthoexciton-to-paraexciton conversion time is 3 ns, leaving only a 0.2 to 3 ns time window for observation of the two-body decay process. The result was $A=7^{+7}_{-3.5}\times10^{-17}$ cm^3/ns, which is nearly identical to the value we measure for thermalized excitons at 70 K. Since the relative orthoexciton and paraexciton populations are changing radically over this wide temperature range, these two results suggest that the individual A^{ij} Auger decay constants are nearly equal and indeed independent of or weakly dependent on temperature.

Let us emphasize at this point that our data (e.g., Fig. 9) unequivocally show a decay rate that depends on the density of the exciton gas. This statement could not be made for experiments at a lattice temperature of 2 K because the kinetic energy of the orthoexcitons was also changing significantly during the nonexponential decay process. At all excitation levels in our present experiments, (a) the average kinetic energy of the excitons over the measurement period is effectively unchanging and (b) the diffusion of excitons out of the initial excitation volume is minimal.

How do these results impact the conclusions of previous work in this area? In order to produce high excitation densities (typically $G_0=10^{20}$ photons absorbed per cm^3 per ns) many experiments have been performed with tightly focused Ar^+ pulses with 10-ns pulse length and 3-μm absorption length. An Auger constant of 6×10^{-17} cm^3/ns implies that the density achieved in such a pulse, neglecting diffusion, is

$$n_{\max}=\sqrt{G_0/A}=1.3\times10^{18} \text{ excitons/cm}^3 \tag{9}$$

and that the effective lifetime of the excitons during the pulse is

$$t_{\min}=(An)^{-1}=0.013 \text{ ns}. \tag{10}$$

In fact, the distributions of excitons and their lifetimes are more complicated than indicated in this simple estimate due to diffusion and the effect of Auger decay on the spatial distribution, as indicated in Sec. II. A computation that takes into account all of these factors will be reported in a later paper.[22] Nevertheless, the simple estimate above shows that the Auger constant is effective in preventing densities of 10^{19}–10^{20}/cm^3 that were reported earlier in the context of Bose Einstein statistics. It is significant that the temperature used in the present experiment, $T=70$ K, is comparable to the Auger-induced temperatures in those earlier experiments, making the present measurements all the more relevant. The two-body decay process—Auger recombination—is a powerful limiting process that makes the thermodynamic condensation of excitons in Cu_2O a remote possibility.

In conclusion, we have measured a strong two-body decay rate for excitons in cuprous oxide at 70 K. At moderate exciton densities the two-body decay rate in Cu_2O is strong enough to compete with other kinetic processes, and provides important constraints on the achievable densities of excitons. The corresponding Auger-heating effect plays an important role in the thermalization of the kinetic energy of excitons, which we believe is the key to understanding the quantumlike energy distributions at high densities, the subject of a subsequent paper.

ACKNOWLEDGMENTS

This work was supported by the National Science Foundation Grant No. DMR92-07458 and by the MRL Laser Laboratory under DOE Grant No. DEFG02-96ER45439.

[1] A. Mysyrowicz, D. Hulin, and C. Benoit à la Guillaume, J. Lumin. **24**, 629 (1981).
[2] C. D. Jeffries and L. V. Keldysh, *Electron-Hole Droplets in Semiconductors* (North-Holland, Amsterdam, 1983).
[3] P. L. Gourley and J. P. Wolfe, Phys. Rev. B **24**, 5970 (1981).
[4] For an early review of Cu_2O properties, see V. T. Agekyan, Phys. Status Solidi A **43**, 11 (1977).
[5] See, for example, the review by J. P. Wolfe, J. L. Lin and D. W. Snoke, in *Bose-Einstein Condensation*, edited by A. Griffin, D. W. Snoke, and S. Stringari (Cambridge University Press, Cambridge, 1995), p. 281.
[6] N. Naka, S. Kono, M. Hasuo, and N. Nagasawa, Prog. Cryst. Growth Charact. **33**, 89 (1996).
[7] T. Goto, M. Y. Shen, S. Koyama, and T. Yokouchi, Phys. Rev. B **55**, 7609 (1997).
[8] D. Hulin, A. Mysyrowicz, and C. Benoit à la Guillaume, Phys. Rev. Lett. **45**, 1970 (1980).
[9] D. W. Snoke, J. P. Wolfe, and A. Mysyrowicz, Phys. Rev. Lett. **59**, 827 (1987).
[10] K. E. O'Hara, L. Ó Súilleabháin, and J. P. Wolfe, Phys. Rev. B **60**, 10 565 (1999).
[11] K. E. O'Hara, J. R. Gullingsrud, and J. P. Wolfe, Phys. Rev. B **60**, 10 872 (1999).
[12] F. I. Kreingol'd and V. L. Makarov, Fiz. Tverd. Tela (Leningrad) **15**, 1307 (1973) [Sov. Phys. Solid State **15**, 890 (1973)].
[13] N. Caswell and P. Y. Yu, Phys. Rev. B **25**, 5519 (1982); J. S. Weiner, N. Caswell, P. Yu, and A. Mysyrowicz, Solid State Commun. **46**, 105 (1983).
[14] D. Snoke, D. P. Trauernicht, and J. P. Wolfe, Phys. Rev. B **41**, 5266 (1990).
[15] G. M. Kavoulakis, G. Baym, and J. P. Wolfe, Phys. Rev. B **53**, 7227 (1996).
[16] The sample is immersed in liquid nitrogen. We cool the liquid to 69 K by pumping the nitrogen vapor down to 250 torr and then repressurizing the cryostat with helium gas. The liquid nitrogen then evaporates, rather than boiling, and remains below 71 K for the duration of the experiment.
[17] Due to the forbidden direct gap, the radiative lifetime of the orthoexciton via a phonon-assisted process is about 14 μs, and the corresponding radiative lifetime of the paraexcitons is 500 times longer.
[18] D. P. Trauernicht and J. P. Wolfe, Phys. Rev. B **33**, 8506 (1986).
[19] B. Karlsson, C. G. Ribbing, A. Roos, E. Valkonen, and T. Karlsson, Phys. Scr. **25**, 826 (1982).
[20] If the absorption through the crystal were not taken into account, an exciton gas temperature of 50 K would be incorrectly derived from a fit to the data.
[21] J. L. Lin and J. P. Wolfe, Phys. Rev. Lett. **71**, 1222 (1993).
[22] K. E. O'Hara and J. P. Wolfe (unpublished).